BOUNDARY ELEMENT METHOD FOR RAYS IN PLATES

A. Le Bot, V. Cotoni

Laboratoire de Tribologie et Dynamique des Systèmes
École Centrale de Lyon
36, av. Guy de Collongue
Lyon, FRANCE

ABSTRACT

This paper is devoted to the study of the propagation of rays inside plates. The theoritical formalism is based upon energy variables of the whole vibrating field rather than magnitude and direction of individual rays. It yields some equations of integral type which are numerically solved with the boundary element method. The software CeReS has been especially designed to solve these equations. Some experiments on highly damped plates with non diffuse field are presented and discussed.

NOMENCLATURE

W	vibrating energy density, J/m^2
$\mathbf{I}$	energy flow vector, W/m
ω	frequency, rad/s
c	group velocity, m/s
α	subscript for type of wave
m	absorption factor, m^{-1}
η	damping loss factor

1 INTRODUCTION

Few methods are available for the problem of vibrating assembled plates in high frequency range. The most common is SEA [1]. Alternative methods have been proposed to improve SEA and particularly to predict the repartition of vibrational energy inside subsystems. On that subject, let mention the work of Nefske and Sung [2] where an analogy with the thermal conduction in material is developped. Nevertheless, this analogy is subjected to some limitations that have been emphasized in literature [3−7]. In order to avoid these difficulties, this paper proposes a method rather based on energy transfer by rays. The first part of this text is intended for theoritical aspects of the method. The underlying equations are numerically solved with the help of a software, called CeReS that has been specifically designed for applications in vibroacoustics. At last, an experiment on a build-up structure made of assembled plates were carried out and the results have been compared with the results of the numerical model provided by the software CeReS.

2 GENERAL CONCEPTS

The analysis of vibrating fields in the high frequency range requires us to consider several concepts which are discussed in this section.

2.1 TRAVELING WAVE

We define high frequencies as the domain where at least several wavelengths lie in the system or, in other words, the characteristic length of the structure is much greater than the wavelength. When several subsystems are connected, the validity domain must be restricted. All subsystems must be separately in the high frequency band and thus high frequencies for the whole structure begin when several wavelengths lie in each subsystem.

Any vibrating field may be viewed as a linear superposition of some traveling waves. The reasons of this choice instead of a modal decomposition is that the only relevant phenomenon in the high frequency range is the *energy transfer between any parts of the structure.*

The first step in developing our model is to make an exhaustive list of all kinds of wave which can propagate inside plates. As we are concerned with some wavelengths which are much greater than the thickness of plates, the conventional theory of Love plates remains valid. It is well-known that three kinds of traveling waves may exist in an infinite extended Love plate. The first type is the bending wave responsible of out-of-plane motion. All quantities attached to this wave will be noted with a subscript b. The second and third types of wave are the longitudinal and transverse waves for in-plane motion with sub-

scripts l and t. The corresponding group velocities are denoted by c_α where $\alpha = b, l$ or t.

The fact that in the absence of curvature, all waves propagate independently of each other leads to a major simplification in describing vibrating field with a wave approach. No energy exchange takes place inside plates during propagation. The only way for a wave to exchange some energy with other kinds of wave is by reflection on a boundary. Of course this phenomenon usually called conversion mode must be taken into account in our model.

In what follows, the energy attached to evanescent waves will be systematically neglected when evaluating the vibrating energy inside the structure and the energy flow of these waves will not affect the energy balance at any point. But these waves must be accounted for evaluating the local energy efficiencies that drive energy exchange between traveling waves at connections of plates.

2.2 WAVE-PACKET

Each time we shall be interested in transient aspects of the dynamical behavior of systems, the traveling wave description will turn out to be unappropriate. It appears that for the purpose of accounting for time-dependance while staying in the high frequency domain, the most natural generalization of traveling waves is the wave-packet concept. Wave-packet may be thought as a traveling wave of finite duration, or, in other words, a traveling wave amplitude-modulated by a pulse shaped waveform, which initially restricts the wave-packet to a finite spatial spread. The duration of the disturbance must be large compared with the period of the main oscillation such that the wave-packet comprises several cycles. The high frequency assumption then just states that the frequency ω of oscillation within the packet lies in the high frequency domain, that is the wavelength is smaller than a characteristic length of the system. In order that wave-packets behave like traveling waves during their passing, we must also add the assumption that the shape function varies slowly compared with the main oscillation.

2.3 SOME PRINCIPLES FOR HIGH FREQUENCIES

With these aspects in mind, we now turn to the description of the dynamical behavior of both traveling waves and wave-packets. All the material necessary in what follows may be summarized in three principles.

The first principle stems from the integral formulation of vibrating plate problem. The underlying idea of these integral representation formulae is that at any point *the vibrating field is the linear superposition of, on the one hand, the direct field emerging from actual sources and, on the other hand, the diffracted field or scattered field emerging from secondary sources located on boundary.* For purposes which follow, the relevant fact is that any vibrating field may be synthetised by summing traveling waves or wave-packets whose sources are clearly identified, driving points, boundaries, interfaces and, more generally, any point where interaction of waves occurs. The application of this principle that will be referred to as the *diffraction principle*, will turn out to be a powerful tool allowing a prediction of energy fields.

The second postulate states that *all traveling waves and wave-packets are uncorrelated* that is the relative phase between an arbitrary pair of waves is a uniform random variable. In view of the first principle, it should be distinguished between uncorrelation of actual sources and secondary sources. The first type is a physical assumption in the sense that it must be checked on the actual experiment that driving forces or moments are effectively uncorrelated. In opposition, uncorrelation of diffraction sources or mixed sources rather results from an approximation deliberately introduced in the description of deterministic systems. The consequences of this lost of information will be highlighted in view of results of applications later discussed.

Finally, the third and last principle is the *locality principle* which may be enounciated in these words. *Any interaction process involving several waves interacting at a given point just depends on local geometry of system and wavefronts.* The most fundamental interest of locality principle lies in the fact that it allows the substitution of any problem of interacting waves by a canonical problem with identical local geometry but extrapolated in such a manner that a closed-form solution is accessible.

3 ENERGY TRANSFER

3.1 ENERGY FIELDS

In this text, vibratory fields are fully described with the help of two energy variables, namely the energy density $W_\alpha(M,t)$, a scalar quantity and the energy flow $\mathbf{I}_\alpha(M,t)$, a vector quantity. Both depend on position M and time t. By virtue of the uncorrelation assumption, all energy quantities are additive that is *linear superposition is valid for energy variables*. In particular, energy variables have to be the sums of related energies attached to individual waves.

At any point M and any time t, the energy balance equation is:

$$\mathbf{div}.\mathbf{I}_\alpha + p_\alpha^{\mathrm{diss}} + \frac{\partial W_\alpha}{\partial t} = \rho_\alpha \quad \alpha = b, l \text{ or } t \tag{1}$$

where p_α^{diss} is the power density being dissipated, ρ_α is the power density being injected by driving forces and $\partial W_\alpha / \partial t$ is the time-varying term of energy density. Of course power density being injected is assumed to be known, or at least, may be derived from imposed force or displacement.

In general systems, energy of waves should decay during propagation due to the action of damping phenomena. In the present text, we shall call damping all processes of conversion of the vibrational energy into a form of energy which is not taken into account, including heat, sound and so on. The nature of physical processes responsible of dissipation, in sense of the above definition, may be of various kinds. Viscous forces applied to structure by a surrounding fluid, internal friction forces, friction at interfaces of metal sheets of built-up structures, acoustic radiation of boundaries are some examples of such processes. We adopt a universal damping law for internal losses. A wave of energy flow magnitude I_α, after traversing a thickness ds in its direction of propagation, will be weakened in such a way that $dI_\alpha = \eta\omega W_\alpha ds$ where ω is the circular frequency of the wave and η an appropriate damping loss factor. Sometimes, it should be more convenient to use a rather acoustical notation by introducing an absorption factor m defined by $dI_\alpha = mc_\alpha W_\alpha ds$. The power density being dissipated is then related to the energy density by:

$$p_\alpha^{\text{diss}}(M,t) = \eta\omega W_\alpha(M,t) = mc_\alpha W_\alpha(M,t) \tag{2}$$

Let us calculate energy fields for pure traveling waves. The application of the diffraction principle requires the knowledge of the direct field, that is the energy density created by a point source in an infinitely extended medium. This energy density is noted $G_\alpha(S,\tau;M,t)$ where S is the source point sending up a signal at time τ and M is the observation point at time t. The related energy flow is noted $\mathbf{H}_\alpha(S,\tau;M,t)$. Sometimes, we shall use the notation H_α for the magnitude of the energy flow vector. The power balance to be verified is:

$$\mathbf{div}_M.\mathbf{H}_\alpha + mc_\alpha G_\alpha + \frac{\partial G_\alpha}{\partial t} = \delta_S(M)\delta_\tau(t) \tag{3}$$

for an impulse excitation. But for a pure traveling wave, G_α and H_α must be related by the relationship:

$$H_\alpha = c_\alpha G_\alpha \tag{4}$$

The outgoing solution of (4) and (3) is found to be:

$$G_\alpha(S,\tau;M,t) = G_\alpha(S;M)\delta(t-\tau-SM/c_\alpha) \tag{5}$$
$$\mathbf{H}_\alpha(S,\tau;M,t) = \mathbf{H}_\alpha(S;M)\delta(t-\tau-SM/c_\alpha) \tag{6}$$

where the steady state solutions $G_\alpha(S;M)$ and $\mathbf{H}_\alpha(S;M)$ has been introduced (see Appendix B of Ref. [8])

$$G_\alpha(S;M) = \frac{e^{-mSM}}{2\pi c_\alpha SM} \tag{7}$$
$$\mathbf{H}_\alpha(S;M) = c_\alpha G_\alpha(S;M)\mathbf{u}_{SM} \tag{8}$$

where $\mathbf{u}_{SM}$ is the unit vector from S toward M. Note that these expessions has been derived under the assumption that m and c_α are constant or, in other words, *that the space of propagation is homogeneous and isotropic.*

By virtue of linear superposition of energy and the diffraction principle, the case of complete wave fields is handle by adding direct fields emerging from primary sources $\rho_\alpha(S,\tau)$ and from secondary sources that will be noted $\sigma_\alpha(P,\mathbf{u},\tau)$ where P belongs to the boundary $\partial\Omega$, $\mathbf{u}$ a direction and τ the time. It results in:

$$W_\alpha(M,t) = \int_\Omega \rho_\alpha(S,t-SM/c_\alpha)G_\alpha(S;M)dS + \int_{\partial\Omega} \sigma_\alpha(P,\mathbf{u}_{PM},t-PM/c_\alpha)G_\alpha(P;M)dP \tag{9}$$

A similar relationship is obtained for energy flow:

$$\mathbf{I}_\alpha(M,t) = \int_\Omega \rho_\alpha(S,t-SM/c_\alpha)\mathbf{H}_\alpha(S;M)dS + \int_{\partial\Omega} \sigma_\alpha(P,\mathbf{u}_{PM},t-PM/c_\alpha)\mathbf{H}_\alpha(P;M)dP \tag{10}$$

Of course primary sources ρ_α are assumed to be known but the layer σ_α remains unknown and an additional equation has to be sought to determine it.

Boundary is assumed to be a perfectly diffuse reflector. It then leads to a directional emitted flux $\sigma_\alpha(P,\mathbf{u},t)/2\pi$ which varies with the cosine of the polar angle θ_P. We then write:

$$\sigma_\alpha(P,\mathbf{u},t) = \sigma_\alpha(P,t)\cos\theta_P \tag{11}$$

This is the Lambert's law.

3.2 REFLECTION ON BOUNDARIES

The required equation on σ_α is found by applying the power balance at any point P on the boundary $\partial\Omega$.

We define the *directional hemispherical reflectivity* $R_{\beta\alpha}(\mathbf{v})$ of a surface dP as the total reflected energy flux leaving dP into all directions due to the directional incident flux from direction $\mathbf{v}$. The directional reflectivity is also called *reflection efficiency*. This is the ratio of the reflected power of the wave α over the incident power of the wave β and, thus, its value runs from 0 to 1.

The total energy flux leaving dP is found to be $\sigma_\alpha(P,t)/\pi$. It is obtained by summing all the contributions of directions $\mathbf{v}$ and types β of wave. So,

$$\frac{1}{\pi}\sigma_\alpha(P,t) = \sum_\beta \int R_{\beta\alpha}(\mathbf{v})\mathcal{P}_\beta(P,\mathbf{v},t)dv \tag{12}$$

where $\mathcal{P}_\beta(P,\mathbf{v},t)$ is the incident flux per unit angle of a wave β from the incident direction $\mathbf{v}$. The integration runs over all incident angles.

The infinitesimal incident flux $\mathcal{P}_\beta(P,\mathbf{v},t)dv$ at P stemming from $\mathbf{v}$ is given by:

$$\mathcal{P}_\beta(P,\mathbf{v},t)dv = [\int_{(P,dv)} \rho_\beta(S,t-SP/c_\beta)H_\beta(S,P)\mathbf{v}dS + \sigma_\beta(Q,\mathbf{v},t-QP/c_\beta)H_\beta(Q,P)\mathbf{v}dQ].\mathbf{n}_P \tag{13}$$

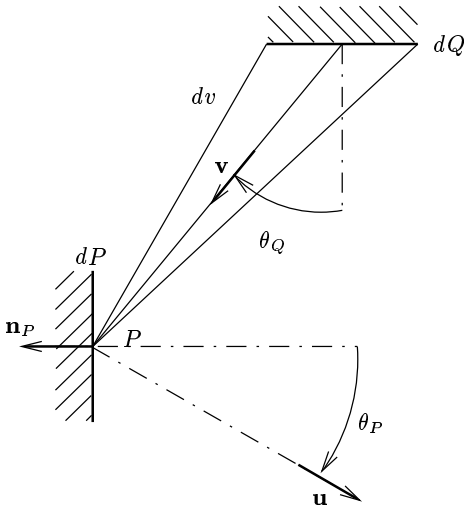

Figure 1: Incident flux at a point P of the boundary stemming from the solid angle dv about $\mathbf{v}$.

where $\mathbf{n}_P$ is the outward unit normal to the boundary at P and the integration is performed over the cone (P, dv) of vertex P and angle dv. Notations are defined in Fig. 1.

By substituting (13) into Eq. (12), we obtain an integral equation on $\sigma_\alpha(P,t)$.

$$\frac{1}{\pi}\sigma_\alpha(P,t) = \sum_\beta \left[\int_\Omega R_{\beta\alpha}(\mathbf{u}_{SP})\rho_\beta(S, t - SP/c_\beta)\mathbf{H}_\beta(S,P)dS + \int_{\partial\Omega} R_{\beta\alpha}(\mathbf{u}_{QP})\sigma_\beta(Q, t - QP/c_\beta)\cos\theta_Q \mathbf{H}_\beta(Q,P)dQ\right].\mathbf{n}_P \quad (14)$$

This integral equation fully determines the unknowns σ_α.

3.3 TRANSMISSION AT INTERFACES

The analysis of reflection and transmission at the interface between two media or more, is relatively straightforward, following a similar way as in the previous section. All quantities are labelled with a subscript i referring to the medium that is considered. For instance, at any point P belonging on the interface, $\sigma_{i,\alpha}/\pi$ denotes the total emitted flux towards the medium i.

Now the reflection condition (12) is replaced by some transmission conditions. It is tacitly assumed that reflection is the particular case of transmission from a system to itself. Thus, the transmission conditions read:

$$\frac{1}{\pi}\sigma_{i,\alpha}(P,t) = \sum_{j,\beta}\int R_{ji,\beta\alpha}(\mathbf{v},)\mathcal{P}_{j,\beta}(P,\mathbf{v},t)dv \quad (15)$$

There are as many equations as types α of wave and systems i connected at P. Further, we explicit the different terms in the same way than for the reflection condition in the previous section. It yields:

$$\frac{1}{\pi}\sigma_{i,\alpha}(P,t) = \sum_{j,\beta} \left[\int_{\Omega_j} R_{ji,\beta\alpha}(\mathbf{u}_{SP})\rho_{j,\beta}(S, t - SP/c_\beta)\mathbf{H}_{j,\beta}(S,P)dS + \int_{\partial\Omega_j} R_{ji,\beta\alpha}(\mathbf{u}_{QP})\sigma_{j,\beta}(Q, t - QP/c_\beta)\cos\theta_Q \mathbf{H}_{j,\beta}(Q,P)dQ\right].\mathbf{n}_P \quad (16)$$

This is the set of integral equations corresponding to diffuse transmission. This set has been derived in Ref. [8] for two plates in steady state condition for a solely type of wave.

3.4 NON-CONVEX DOMAIN

Until now, we have tacitly assumed that the domain of energy propagation is convex. However, such an assumption is no longer necessary.

We must consider that the energy emanating from an actual source S or a boundary source Q cannot reach a point M if an obstacle is encountered on its path. In such a case, the energy is reflected and/or absorbed by the obstacle. This secondary emission of energy is yet accounted for by putting a boundary source on the obstacle.

Thus, Eqs. (9,10) must be modified in such a way that only the sources S and Q visible by the point M have to be accounted for. In the same way, Eqs. (14,16) must also be modified. A simple way to discard these hidden sources is to multiply Eqs. (7,8) of direct fields by a visibility function $V(S,M)$ which value is one when S is visible from M and zero otherwise.

4 DESCRIPTION OF THE SOFTWARE CERES

The software CeReS has been designed to solve Eqs. (14,16) for some cases. In Ref. [9], results for acoustical enclosures has been compared with results of a ray-tracing software in steady state conditions. It results in a good agreement. In this text, we are rather interested in structures made of assembled plates.

Each plate is defined as a part of plane surrounded by a polygonal line. The plates are convex or not. These plates are joined by their edges. The joints may be composed of an arbitrary number of plates. The geometry of the plates as well as the constitution of the joints must be specified to the software in a special data file. The structure then obtained may be subjected to some point loadings. These sources are described in terms of their positions and the powers ρ_α being injected into any kind α of waves. The response may be computed at any point of any plate.

The damping occurs in two ways. On the one hand, a damping loss factor η is attached to each plate. It is responsible of the decrease of energy during propagation. On the other

hand, an absorption factor α is attached to each edge of each plate. It is responsible of the absorption of the energy when waves impinge on the boundary. In the software CeReS, the reflection efficiencies are evaluated on the basis of the equilibrium of forces and moments at the interface as well as the continuity of displacements. These considerations leads to non-dissipative reflection efficiencies, that is the sum equals unity. To take into account extra-damping which may occurs at edges or interfaces, the user can specify the absorption factor α for each edge. Reflection efficiencies theoritically predicted are then multiplied by this factor.

The software CeReS solves Eqs. (14,16) in steady state conditions. In this matter, a boundary element method is applied. Each edge of plates is divided into a limited number of elements of equal size. The magnitudes σ_α of the boundary sources are assumed to be constant over each boundary element. Thus, three unknowns σ_α, $\alpha = b, l$ or t are attached to each boundary element. For each element, Eqs. (14) or (16), depending on the position of the element at edge or interface, is applied at the middle of the element. Thus, the set of Eqs. (14,16) leads to a system of linear equations on this unknowns σ_α. The coefficients involved are some integrals evaluated by the Gauss quadrature. It should be pointed out that these integrals are regular unlike the singular integrals involved in the classical boundary element method, allowing a fast and accurate computation. This linear system is solved with a Lapack routine. Once the source magnitudes σ_α are computed, the energy density or energy flow inside each plate is evaluated from Eqs. (9,10).

The next section is devoted to the comparison of some results of the software CeReS with some measurements achieved on a structure.

5 EXPERIMENTAL RESULTS

The first experimentation deals with a U-shaped aluminium plate. The thickness is 1.5 mm and the plate is covered with a damping material in order to avoid a diffuse field. It is assumed that the presence of the damping material affects the damping ratio and the surfacic mass but not the bending rigidity of the aluminium plate. The surfacic mass of the plate is $\rho = 5.2\ \mathrm{kg/m^2}$. The damping ratio is $\eta = 15\%$ over all octave bands of interest and was measured on a piece of square plate (with the same damping material) excited by a shaker which injected power was known. The U-plate was excited by two shakers. The RMS cross-spectrum force-acceleration $S_{fa}(\omega)$ for each driving point was measured with some impedance heads located between the structure and shakers. The power being injected into an octave band was determined with a frequency-integration of the cross-spectrum $P_{inj} = \Re \int_{\omega_0/\sqrt{2}}^{\omega_0\sqrt{2}} S_{fa}(\omega)/(i\omega) d\omega$. Their values are summarized in Tab. 1. The RMS power spectral density $S_{vv}(\omega)$ of velocity was measured with a velocimeter at several points on a single line (see Fig. 2 for the experimental setup and the measurement line). The energy density contained in four octave bands was easily determined from velocities assuming that it is two times the kinetic energy $W_{meas} = \rho \int_{\omega_0/\sqrt{2}}^{\omega_0\sqrt{2}} S_{vv}(\omega) d\omega$. On the other hand the CeReS model acounts for flexural waves solely. Other kinds of waves cannot be created since the structure is flat. The boundary of the plate is divided into 70 elements. The CeReS model thus contains 70 degrees of freedom. Fig. 3 shows some comparisons of the measured energy densities and the prediction of the software CeReS along the line.

	300 Hz	600 Hz	1200 Hz	2400 Hz
$Excitation1$	6.1 mW	4.5 mW	4.5 mW	2.9 mW
$Excitation2$	0.06 mW	0.76 mW	1.0 mW	0.83 mW

TABLE 1: Power being injected by shakers in the U-plate for each octave band.

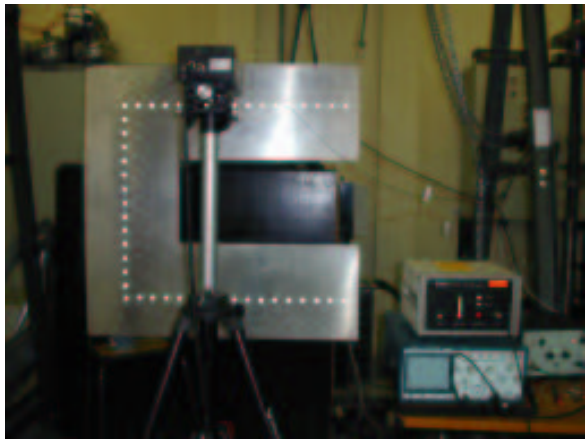

Figure 2: Experiment on a U-shaped plate. View of the experimental setup including the velocimeter and positions of measurement points along a line.

The second experimentation is concerned with a more complex structure. Fig. 4 shows the experimental setup and the geometry of this structure. It is made of seven plates of steel. The thickness is $8/10$ mm and the structure is entirely covered with a damping material named CATANE AL with thickness 1.24 mm and density $1.26\ \mathrm{g/cm^3}$. An equivalent surfacic mass is used considering again that the presence of the damping material does not affect the rigidity of steel plates. The surfacic mass is $\rho = 7.8\ \mathrm{kg/m^2}$ and the damping ratio is $\eta = 2\%$. The same technique of measurement was involved although some accelerometers was used instead of the velocimeter. The CeReS model of this structure take into account all kinds of wave and the structure was discretized with 438 boundary elements and thus the CeReS model contains 1314 degrees of freedom. Fig. 5 shows some comparisons of the measured energy densities in narrow band over $50 - 3200$ Hz and the prediction of the software CeReS at four points.

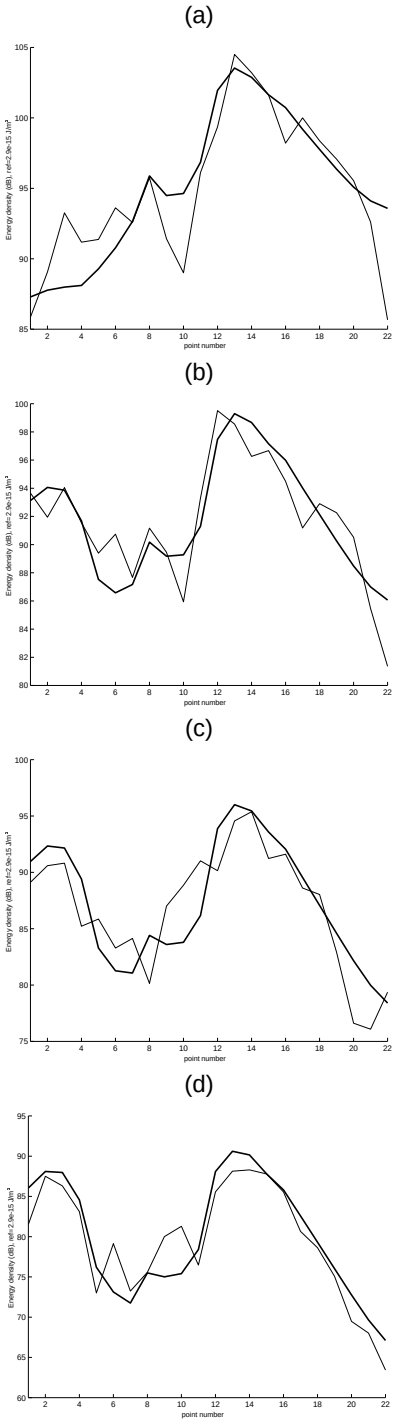

Figure 3: U-shaped plate. Comparison of measured energy density (thin line) and predicted values by the software CeReS (thick line) for the octave band centered at (a) 300 Hz, (b) 600 Hz, (c) 1200 Hz and (d) 2400 Hz.

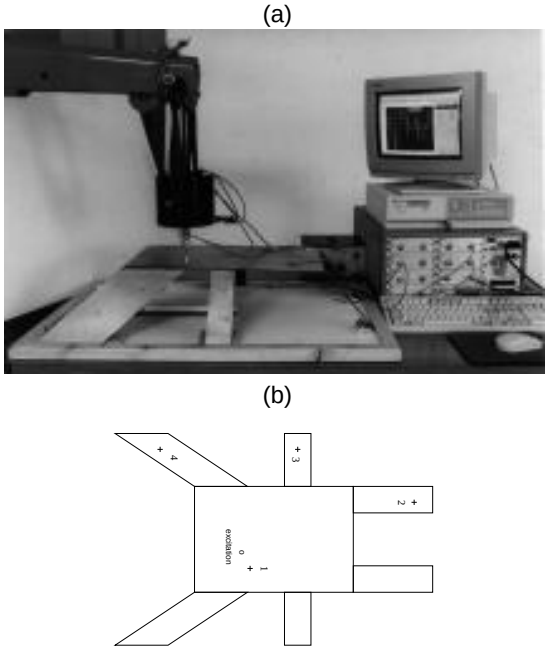

Figure 4: Experiment on a seven-plates structure. (a) View of the experimental setup. (b) Geometry of the structure and position of the driving point and measurement points.

6 CONCLUSION

In this text, we have derived some equations for the study of vibrational energy transfer in plates. These equations have been obtained under the high frequency assumption. The energy is carried out by rays and the energies of each ray are simply summed. Some integral equations on the emitted flux are found. A boundary element method is involved to solve them. The sofware CeReS is especially designed to perform this task. The comparison between numerical results provided be CeReS and measurements achieved on a multi-plate structure, highlights the interest of such an approach.

ACKNOWLEDGEMENTS

The author gratefully acknowledges the Région Rhône-Alpes for his financial support.

REFERENCES

[1] **Lyon, R.**, Statistical Energy Analysis of Dynamical Systems: Theory and Application, Cambridge, Massachusetts, MIT Press, 1975.

[2] **Nefske, D.** and **Sung, S.**, *Power Flow Finite Element Analysis of Dynamic Systems: Basic Theory and Application to Beams*, NCA Publication, Vol. 3, 1987.

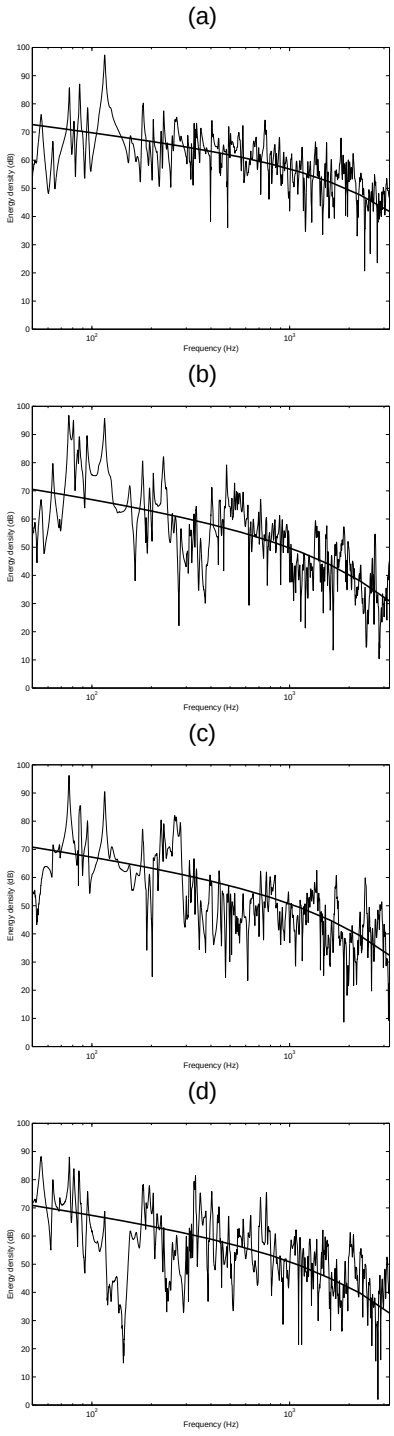

Figure 5: Seven-plates structure. Comparison of measured energy densities in narrow band (thin line) and predicted RMS-values (thick line) by the software CeReS at (a) point 1, (b) point 2, (c) point 3 and at (d) point 4.

[3] **Langley, R.**, *On the Vibrational Conductivity Approach to High Frequency Dynamics for Two-dimensional Structural Components*, Journal of Sound and Vibration, Vol. 182, pp. 637–657, 1995.

[4] **Carcaterra, A.** and **Sestieri, A.**, *Energy density equations and power flow in structures*, Journal of Sound and Vibration, Vol. 188(2), pp. 269–282, 1995.

[5] **Le Bot, A.**, *Geometric diffusion of vibrational energy and comparison with the vibrational conductivity approach*, Journal of Sound and Vibration, Vol. 212(4), pp. 637–647, 1998.

[6] **Carcaterra, A.** and **Adamo, L.**, *Thermal analogy in wace energy transfer: theoritical and experimental analysis*, Journal of Sound and Vibration, Vol. 226(2), pp. 253–284, 1999.

[7] **Ichchou, M. N., Le Bot, A.** and **Jezequel, L.**, *A transient local energy approach as an alternative to transient SEA: wave and telegraph equations*, Submitted to Journal of Sound and Vibration, to be published.

[8] **Le Bot, A.**, *A vibroacoustic model for high frequency analysis*, Journal of Sound and Vibration, Vol. 211(4), pp. 537–654, 1998.

[9] **Le Bot, A.** and **Bocquillet, A.**, *Comparison of an integral equation on energy and the ray-tracing technique for room acoustics*, Journal of Acoustical Society of America, Vol. 108(4), pp. 1732–1740, 2000.